RESEARCH ARTICLE

Strength, microstructure, and thermal conductivity of the insulation wallboards prepared with rice husk fiber and recycled concrete aggregates

Xiaoniu Yu *, Linzhu Sun*

College of Architecture and Civil Engineering, Wenzhou University, Wenzhou, China

* xnyu@wzu.edu.cn (XY); 20160088@wzu.edu.cn (LS)

Abstract

This paper intends to evaluate the influence of content of rice husk fiber and cementitious materials on mechanical properties and thermal conductivity of thermal insulation wallboards. Thermal insulation wallboard contained different mass of rice husk fiber was prepared when the weight of cement, fly ash, cellulose ether, naphthalene superplasticizer, and recycled concrete aggregates was equal. Scanning electron microscopy (SEM) shows the internal structure of the insulation wallboards is very dense. Compared to thermal conductivity of blank group (0.9600 W/m·˚C), B2 (0.1997 W/m·˚C) and C2 (0.1810 W/m·˚C) measured by the DRCD-3030 intelligent thermal conductivity tester can meet certain engineering requirements. Average compressive strength, flexural strength, and thermal conductivity of wallboards decreases with content of rice husk fiber increasing when other materials mass are the same. Under the same conditions of curing time and rice husk content, average compressive and flexural strength increase with the increase of the amount of cementitious material.

1. Introduction

Concrete materials in human social and economic development are indispensable. With the progress of society and people's living standards continues to improve. The per capita demand for concrete has increased year by year, indirectly lead to ecological damage, environmental pollution, and other issues become increasingly prominent. Gravel and sand as non-renewable resources have shown a shrink tendency under the huge consumption. To ensure high-quality aggregate supply more difficult, which will inevitably affect the construction and national economic development. With the acceleration of civil engineering construction, huge amounts of construction waste are generated, of which nearly half are waste concrete. The utilization rate of China's construction waste is less than Europe and the United States. Waste concrete make into recycled aggregates, replacing normal natural aggregates has become an important issue, and researched by scientists around the world [1–23].

The use of recycled concrete aggregate as a building material is now gaining popularity in China's construction materials. High-performance concrete, stub columns, and beams can be cast by recycled concrete aggregates, and have good mechanical properties according to literature reported [24–27]. However, few studies have been conducted on the production of thermal insulation wallboards through recycled aggregates according to web of science index. In this paper, thermal insulation wallboards were prepared with recycled concrete aggregate and rice husk fiber. And the structure and morphology of the wallboards were characterized by X-ray diffraction (XRD) analysis and scanning electron microscopy (SEM). The mechanical properties of the specimens were tested using pressure/bending test machine. In actual engineering, materials with a thermal conductivity of less than 0.20 W/m·°C are usually called thermal insulation materials [28–30]. The results show B2 and C2 of specimens can meet the actual engineering of strength requirements.

2. Experiments and methods

2.1. Experimental materials

(1) Cement: The cement used in this experiment was ordinary Portland cement 42.5 (Zhejiang Hongshi Cement CO., LTD, China), as shown in S1 Table. The initial time and final setting time of the cement were 155 and 334 min, respectively. The 3-day compressive strength and flexural strength were 27.8 and 5.2 MPa, respectively. The 28-day compressive strength and flexural strength were 45.5 MPa, and 7.8 MPa, respectively. (2) Fly ash: The fly ash used in this experiment had properties as follows: the thinness (45 μm residue on sieve), water absorption, the loss on ignition, water content, and the sulfur trioxide content were 18.5%, 107%, 5.8%, 0.75%, and 2.6%, respectively. (3) Recycled concrete aggregates: Waste concrete was made into fine aggregate with particle size of less than 3mm through the aggregate crusher in laboratory (Wenzhou construction and demolition waste, China), as shown in S1 Fig. The water absorption of recycled concrete aggregates was 15.19%. (4) Cellulose ether, naphthalene superplasticizer, and rice husk fiber were purchased from Wenzhou Jingheng Chemical Reagents Company, China.

2.2. Experimental mix proportion design

The cement, fly ash, concrete powder, cellulose ether, naphthalene superplasticizer, and rice husk fiber were mixed in different proportions to make different kinds of cement-based materials, as shown in Table 1. The consistency of cement-based slurry was adjusted to about 8CM. According to the number of specimens, the actual amount of different types of test materials was determined, as shown in S2 Table. The test dimensions were 70.7mm×70.7mm×70.7mm, 40mm×40mm×160mm, and 30mm×300mm×300mm for 12 groups. Each group of specimens was four and numbered A1 ~ A4, B1 ~ B4, and C1 ~ C4. Number A1 ~ A4, B1 ~ B4, and C1 ~ C4 were one group, respectively.

2.3. Specimens preparation

The contents of the experimental materials were calculated and measured according to the requirements for mix proportion. Recycled concrete aggregates, cement, fly ash, cellulose ether, naphthalene superplasticizer, and rice husk fiber were sequencely added into a small mortar mixer. The mixer was covered and mixed for 2 min to achieve uniform mixing. A certain amount of running water was added to the mixture, and continued stirring for 3 min. The consistency of all cement-based slurries was adjusted to about 8CM. The cement-based slurry was then poured into a particular mold (70.7mm×70.7mm×70.7mm, 40mm×40mm×160mm,

Table 1. Mass of raw materials.

Number	Total gelling material (g)	Cement (g)	Fly ash (g)	Concrete powder (g)	Cellulose ether (g)	Naphthalene superplasticizer (g)	Rice husk fiber (g)
A1	4285.70	3428.56	857.14	10000	3.21	21.43	0.00
A2	4285.70	3428.56	857.14	10000	3.21	21.43	571.67
A3	4285.70	3428.56	857.14	10000	3.21	21.43	786.04
A4	4285.70	3428.56	857.14	10000	3.21	21.43	1000.00
B1	5384.60	4307.68	1076.92	10000	4.04	26.92	0.00
B2	5384.60	4307.68	1076.92	10000	4.04	26.92	615.38
B3	5384.60	4307.68	1076.92	10000	4.04	26.92	846.15
B4	5384.60	4307.68	1076.92	10000	4.04	26.92	1076.97
C1	6666.70	5333.36	1333.34	10000	5.00	33.33	0.00
C2	6666.70	5333.36	1333.34	10000	5.00	33.33	666.67
C3	6666.70	5333.36	1333.34	10000	5.00	33.33	916.67
C4	6666.70	5333.36	1333.34	10000	5.00	33.33	1166.67

and 30mm×300mm×300mm). Specimens were demolded after 3d, as shown in Fig 1. Putting the specimens to a standard curing room at temperature of 20 ± 1 ˚C and relative humidity of above 95%, and cured for 7, 14, and 28 days.

2.3. Characterization

The phase composition of products was examined by X-ray diffraction (XRD, Bruker D8-Advance, λ = 1.5406Å, Bruker Company, Karlsruhe, Germany). Scanning electron microscope (SEM, JEOL-7800Prime, operating voltage 5 kV, JEOL, Tokyo, Japan) was used to conduct morphological studies of the samples. The compressive strength and flexural strength of specimens was tested through the ordinary compression/bending test machine. The thermal conductivity of the insulation panels was measured by the DRCD-3030 intelligent thermal conductivity tester (DRCD-3030, Shenyang Hexing Company, Shenyang, China), as shown in Fig 2.

3. Results and discussion

3.1. XRD pattern and micro-structure of the specimens

The composition of concrete powder was analyzed through XRD, as shown in Fig 3. Concrete powder components were mainly a mixture of quartz (JCPDS No. 79–1906), calcite (JCPDS No. 86–2334), Dolomite (JCPDS No. 00–0005), and other impurity materials. The composition of waste concrete is different from the river sand and artificial sand. Amorphous cement hydration products cannot be indexed by the jade 5 program. The constituents of thermal insulation wallboards were analyzed through XRD, as shown in

Fig 1. Image of the specimens after demolding.

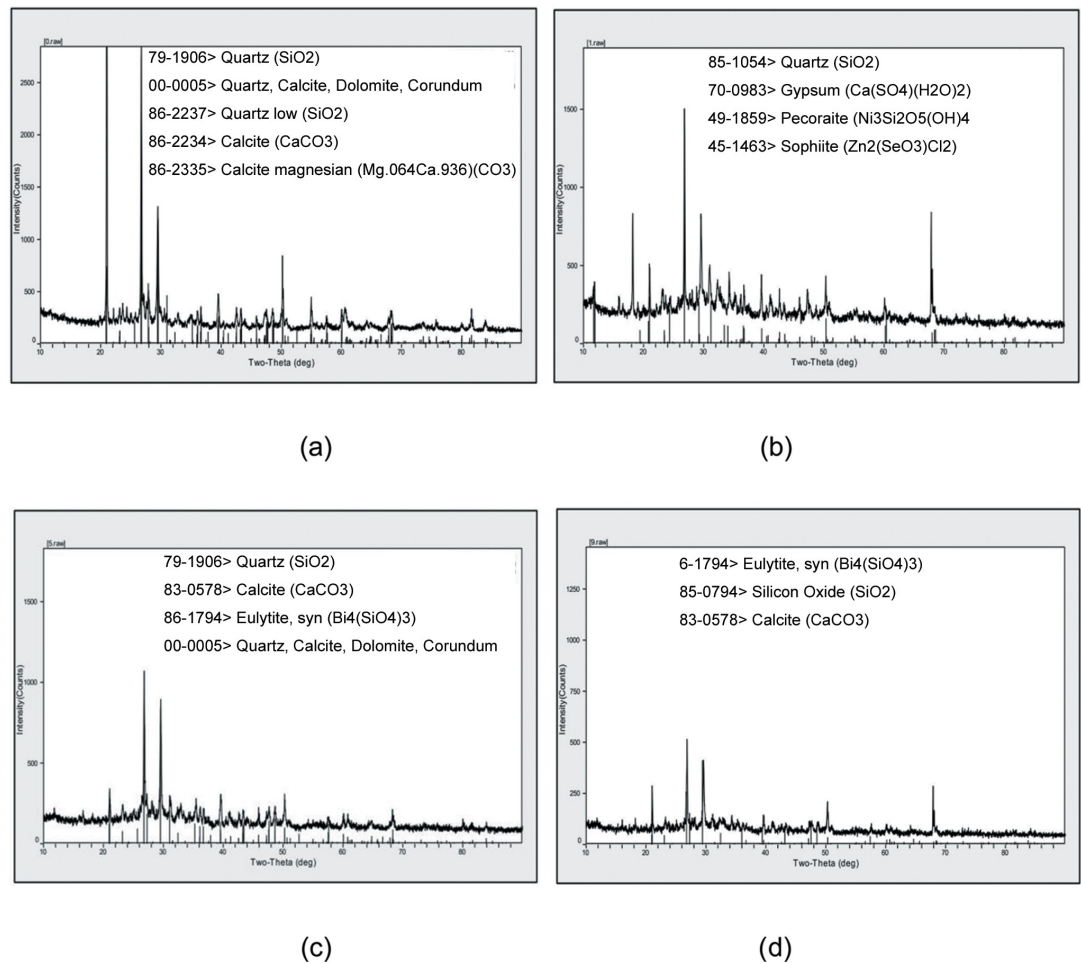**Fig 2. DRCD-3030 intelligent thermal conductivity tester.**

(a)

(b)

(c)

(d)

Fig 3. XRD patterns of the specimens: (a) concrete powder, (b) A1 sample, (c) B1 sample, (d) C1 sample.

PLOS ONE

Preparation of thermal insulation wallboards

o__Aeromonadales|f__Succinivibrionaceae|g__|823406
o__Bacteroidales|f__[Paraprevotellaceae]|g__|2036
o__Bacteroidales|f__[Paraprevotellaceae]|g__CF231|300727
o__Bacteroidales|f__[Paraprevotellaceae]|g__YRC22|325340
o__Bacteroidales|f__|g__|292709
o__Bacteroidales|f__|g__|297576
o__Bacteroidales|f__p-2534-18B5|g__|298963
o__Bacteroidales|f__Prevotellaceae|g__Prevotella|297176
o__Clostridiales|f__|g__|295074
o__Clostridiales|f__|g__|318789
o__Clostridiales|f__|g__|350337
o__Clostridiales|f__|g__|558019
o__Clostridiales|f__Clostridiaceae|g__Clostridium|320863
o__Clostridiales|f__Lachnospiraceae|g__|321902
o__Clostridiales|f__Lachnospiraceae|g__|322505
o__Clostridiales|f__Lachnospiraceae|g__|329746
o__Clostridiales|f__Lachnospiraceae|g__|334956
o__Clostridiales|f__Lachnospiraceae|g__|346525
o__Clostridiales|f__Lachnospiraceae|g__|350041
o__Clostridiales|f__Lachnospiraceae|g__|528266
o__Clostridiales|f__Lachnospiraceae|g__|529873
o__Clostridiales|f__Lachnospiraceae|g__|531773
o__Clostridiales|f__Lachnospiraceae|g__|542096
o__Clostridiales|f__Lachnospiraceae|g__|578649
o__Clostridiales|f__Lachnospiraceae|g__|589852
o__Clostridiales|f__Lachnospiraceae|g__|592572
o__Clostridiales|f__Lachnospiraceae|g__|708680
o__Clostridiales|f__Lachnospiraceae|g__|753891
o__Clostridiales|f__Lachnospiraceae|g__Blautia|341433
o__Clostridiales|f__Lachnospiraceae|g__Clostridium|555445
o__Clostridiales|f__Lachnospiraceae|g__Pseudobutyrivibrio|571031
o__Clostridiales|f__Lachnospiraceae|g__Roseburia|701221
o__Clostridiales|f__Ruminococcaceae|g__Ruminococcus|299609
o__Clostridiales|f__Ruminococcaceae|g__Ruminococcus|554304
o__Clostridiales|f__Ruminococcaceae|g__Ruminococcus|562408
o__Clostridiales|f__Veillonellaceae|g__Anaerovibrio|13805
o__Clostridiales|f__Veillonellaceae|g__Anaerovibrio|663226
o__Clostridiales|f__Veillonellaceae|g__Anaerovibrio|812596
o__Spirochaetales|f__Spirochaetaceae|g__Treponema|297140
o__Spirochaetales|f__Spirochaetaceae|g__Treponema|301587
o__Spirochaetales|f__Spirochaetaceae|g__Treponema|309470
o__Spirochaetales|f__Spirochaetaceae|g__Treponema|332359
o__Spirochaetales|f__Spirochaetaceae|g__Treponema|4335321
o__YS2|f__|g__|340514

Phenyl-butazone Firocoxib

58 44 46
*

Phenylbutazone Firocoxib

Color Key and Histogram
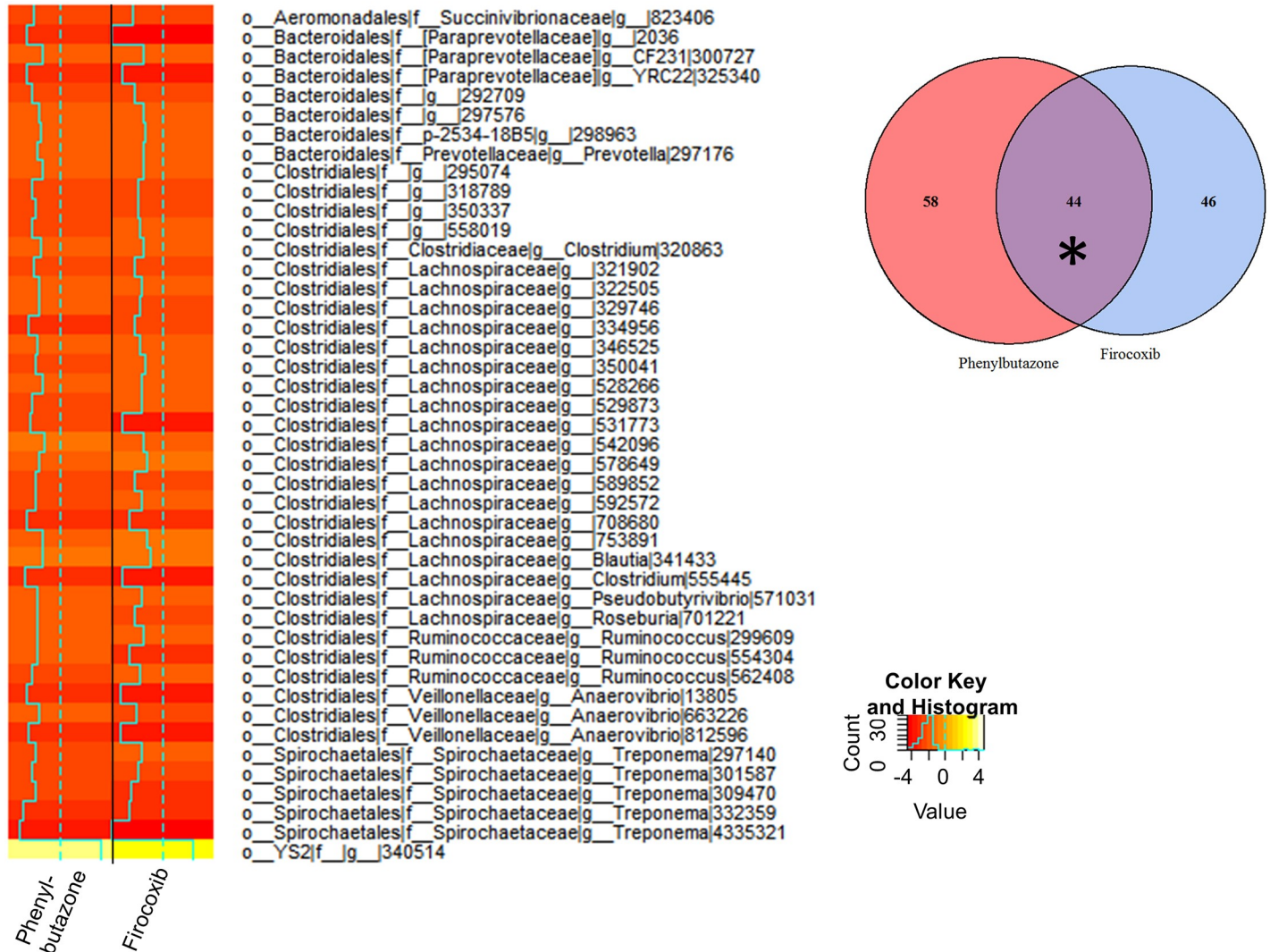
Count

0 30

-4 0 4
Value

Fig 4. SEM images of the specimens: (a, b) concrete powder, (c, d) A1 sample, (e, f) A2 sample, (g, h) A3 sample, (i, j) A4 sample.

Fig 3a, 3b, 3c, and 3d. The XRD results indicated that A1, B1, and C1 samples were mainly a mixture of quartz (JCPDS No. 79–1906), calcite (JCPDS No. 86–2334), and other mineral admixtures. The peaks of quartz and calcite are from concrete powder. The peaks of cement hydration products are too weak and are submerged by the quartz peaks, so it cannot be indexed by the jade 5 program. Therefore, concrete powder mixed with cement can be made into recycled concrete mortar.

SEM images of concrete powder are shown in Fig 4a and 4b. SEM images indicate that shape of concrete powder is irregular block structure and rough surface. SEM images of all types of thermal insulation wall boards were shown by Figs 4, 5, and 6. Cement, concrete powder, rice husk, etc. can be well combined together (Figs 4c, 4e, 4g, 4I, 5a, 5c, 5e, 5g, 6a, 6c, 6e, 6g). The morphology for all types of thermal insulation wall boards is similar to each other. Their morphology is mainly needle-like, flaky, spherical, flocculent, and irregular shape. The results also further confirm the morphology of cement hydration products.
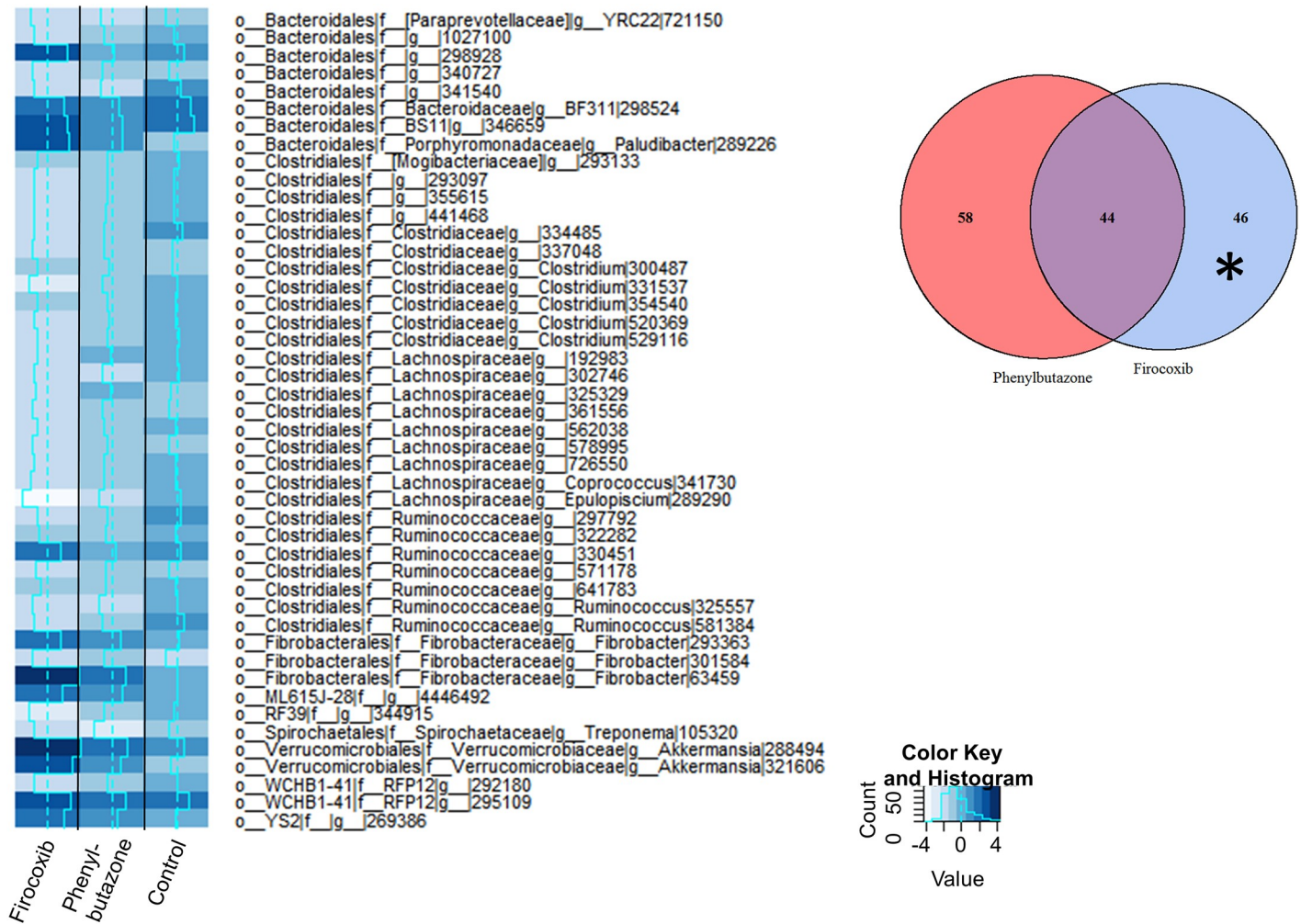
PLOS ONE | https://doi.org/10.1371/journal.pone.0203527 September 19, 2018

5 / 12

o__Bacteroidales|f__[Paraprevotellaceae]|g__YRC22|721150
o__Bacteroidales|f__|g__|1027100
o__Bacteroidales|f__|g__|298928
o__Bacteroidales|f__|g__|340727
o__Bacteroidales|f__|g__|341540
o__Bacteroidales|f__Bacteroidaceae|g__BF311|298524
o__Bacteroidales|f__BS11|g__|346659
o__Bacteroidales|f__Porphyromonadaceae|g__Paludibacter|289226
o__Clostridiales|f__[Mogibacteriaceae]|g__|293133
o__Clostridiales|f__|g__|293097
o__Clostridiales|f__|g__|355615
o__Clostridiales|f__|g__|441468
o__Clostridiales|f__Clostridiaceae|g__|334485
o__Clostridiales|f__Clostridiaceae|g__|337048
o__Clostridiales|f__Clostridiaceae|g__Clostridium|300487
o__Clostridiales|f__Clostridiaceae|g__Clostridium|331537
o__Clostridiales|f__Clostridiaceae|g__Clostridium|354540
o__Clostridiales|f__Clostridiaceae|g__Clostridium|520369
o__Clostridiales|f__Clostridiaceae|g__Clostridium|529116
o__Clostridiales|f__Lachnospiraceae|g__|192983
o__Clostridiales|f__Lachnospiraceae|g__|302746
o__Clostridiales|f__Lachnospiraceae|g__|325329
o__Clostridiales|f__Lachnospiraceae|g__|361556
o__Clostridiales|f__Lachnospiraceae|g__|562038
o__Clostridiales|f__Lachnospiraceae|g__|578995
o__Clostridiales|f__Lachnospiraceae|g__|726550
o__Clostridiales|f__Lachnospiraceae|g__Coprococcus|341730
o__Clostridiales|f__Lachnospiraceae|g__Epulopiscium|289290
o__Clostridiales|f__Ruminococcaceae|g__|297792
o__Clostridiales|f__Ruminococcaceae|g__|322282
o__Clostridiales|f__Ruminococcaceae|g__|330451
o__Clostridiales|f__Ruminococcaceae|g__|571178
o__Clostridiales|f__Ruminococcaceae|g__|641783
o__Clostridiales|f__Ruminococcaceae|g__Ruminococcus|325557
o__Clostridiales|f__Ruminococcaceae|g__Ruminococcus|581384
o__Fibrobacterales|f__Fibrobacteraceae|g__Fibrobacter|293363
o__Fibrobacterales|f__Fibrobacteraceae|g__Fibrobacter|301584
o__Fibrobacterales|f__Fibrobacteraceae|g__Fibrobacter|63459
o__ML615J-28|f__|g__|4446492
o__RF39|f__|g__|344915
o__Spirochaetales|f__Spirochaetaceae|g__Treponema|105320
o__Verrucomicrobiales|f__Verrucomicrobiaceae|g__Akkermansia|288494
o__Verrucomicrobiales|f__Verrucomicrobiaceae|g__Akkermansia|321606
o__WCHB1-41|f__RFP12|g__|292180
o__WCHB1-41|f__RFP12|g__|295109
o__YS2|f__|g__|269386

Firocoxib
Phenyl-butazone
Control

58 44 46
✱

Phenylbutazone   Firocoxib

Color Key and Histogram
Count
50
0
-4 0 4
Value

Fig 5. SEM images of the specimens: (a, b) B1 sample, (c, d) B2 sample, (e, f) B3 sample, (g, h) B4 sample.

https://doi.org/10.1371/journal.pone.0203527.g005

3.2. Influence of the content of rice husk fiber on compressive strength and flexural strength of the specimens

Compressive strength and flexural strength of the specimens in the same age decreasing with the increase of the amount for rice husk fiber when the content of cement, fly ash, concrete powder, cellulose ether, and naphthalene superplasticizer are same, as shown Figs 7 and 8. 7, 14, and 28d of average compressive strength for groups A1 ~ A4 were 6.3, 7.8, and 8.2Mpa, 2.8, 2.8, and 2.9Mpa, 1.9, 2.1, and 2.0Mpa, 1.3, 1.4, and 1.4Mpa, respectively (Fig 7). The average compressive strength of A1 and A2 increased with the increase of curing time and the increase of rice hull content. A1 has the largest growth rate. The average compressive strength of A3 and A4 increased with the increase of curing time and the increase of rice husk content, and the increase was 0.1Mpa. The intensity of 14 ~ 28d was basically maintained constant.

7, 14, and 28d of average compressive strength for groups B1 ~ B4 were 6.5, 9.4, and 10.4Mpa, 3.7, 4.6, and 4.9Mpa, 4.0, 3.7, and 4.0Mpa, 1.9, 2.3, and 2.3Mpa, respectively (Fig 7). Average compressive strength of B1 and B2 increased with the increase of curing time. B1 has the largest growth rate. The average compressive strength of B3 decreased firstly and then increased, and the intensities were the same at 7d and 28d, with the increase of curing time.
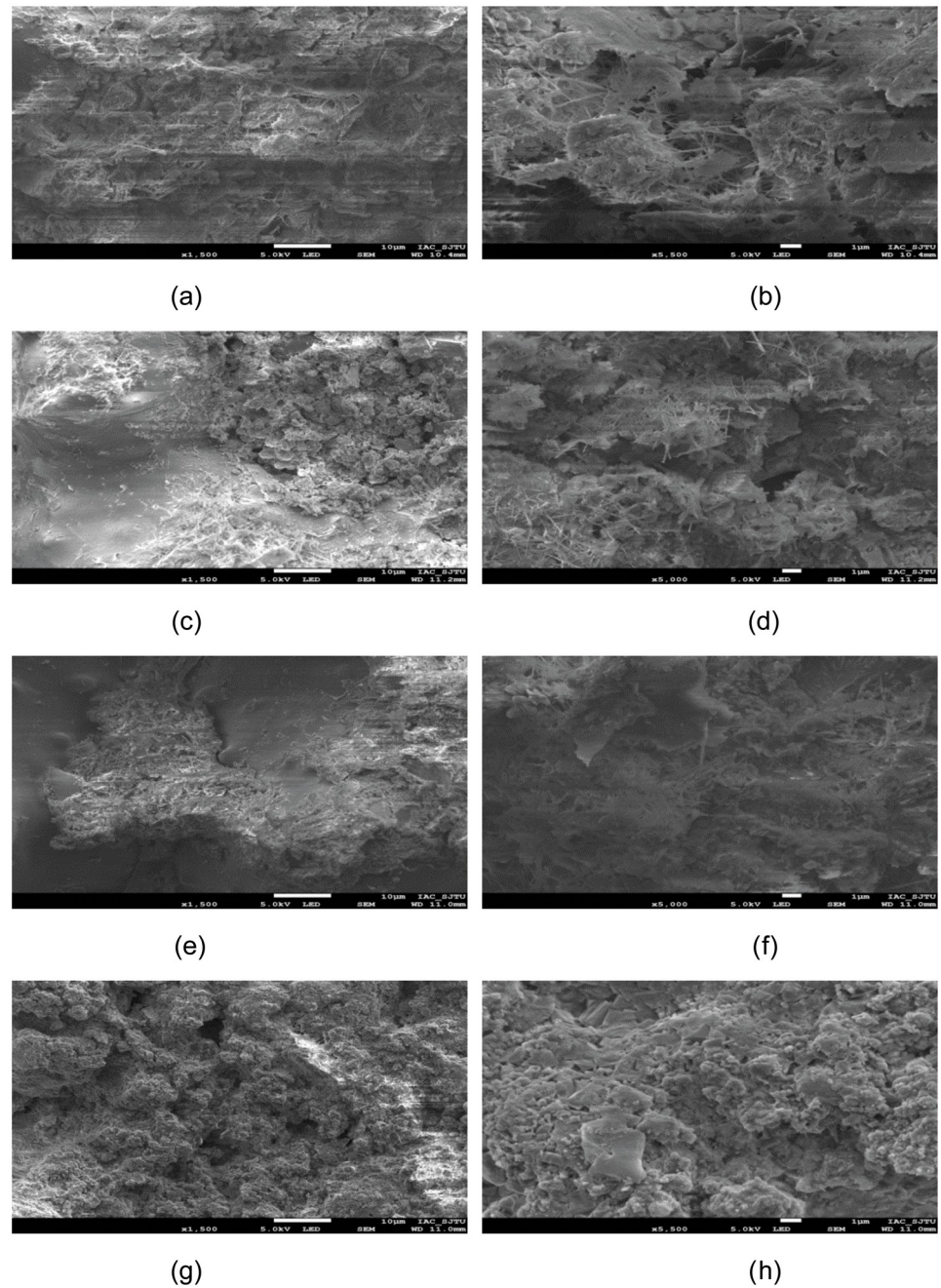
(a)

(b)

(c)

(d)

(e)

(f)

(g)

(h)

Fig 6. SEM images of the specimens: (a, b) C1 sample, (c, d) C2 sample, (e, f) C3 sample, (g, h) C4 sample.

The average compressive strength of B4 was increased by 0.4Mpa at 14 days and the intensity of 14–28 days remained unchanged with the increase of curing time.

For groups C1 ~ C4, average compressive strength at 7, 14, and 28d were 8.0, 13.0, 13.4Mpa, 5.5, 6.7, and 6.6Mpa, 3.5, 4.2, and 3.1Mpa, 2.4, 2.8, and 2.8Mpa, respectively (Fig 7). The average compressive strength of C1 was increased with the increase of curing time, and the growth rate was the largest. With the increase of curing time, the average compressive strength of group C2, C3, and C4 increased corresponding to 7 and 14d, then C2 and C3 were reduced, C4 was maintained.
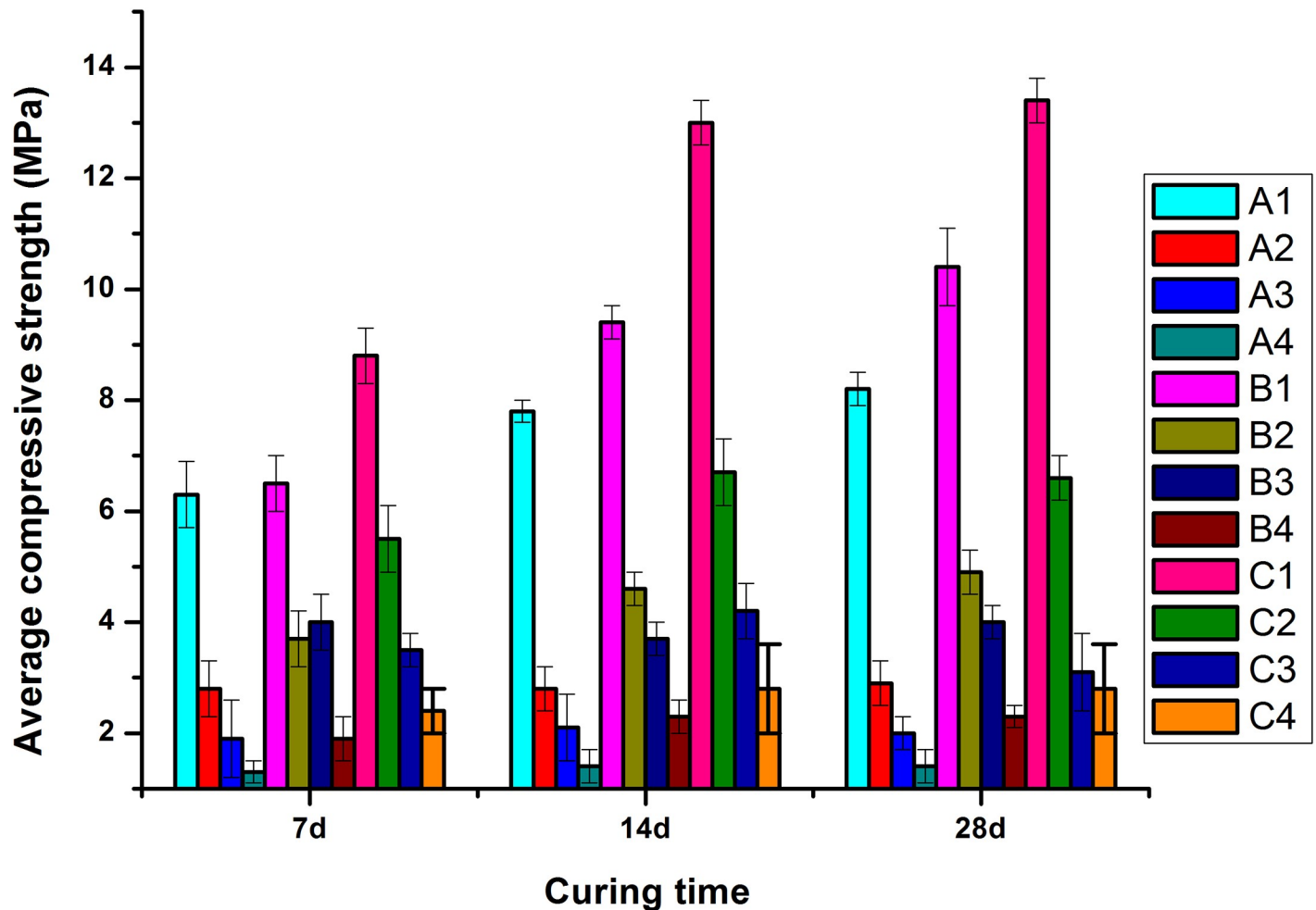
Fig 7. Relationship between curing time and average compressive strength.

For the group numbers A1 ~ A4, 7, 14, and 28d of average flexural strength were 1.7, 3.3, and 3.6Mpa, 1.4, 1.4, and 1.5Mpa, 1.0, 1.0, and 1.1Mpa, 0.8, 0.8, and 0.9Mpa, respectively, as shown in Fig 8. The average flexural strength of groups A1-A4 increases with the increasing curing time and content of rice hull. A1 increases the maximum. The average flexural strength of A2 was maintained at 7 ~ 14d with the increase of curing time.

Fig 8 shows 7, 14, and 28d of average flexural strength of groups B1 ~ B4 were 3.1, 3.3, 3.7Mpa, 1.8, 1.9, and 2.2Mpa, 1.5, 1.8, and 1.7Mpa, 1.1, 1.4, and 1.3Mpa, respectively. Average flexural strength of B1 and B2 increased with the increase of curing time. With the increase of curing time and content of rice husk, average flexural strength of groups B3 and B4 increased.

Average flexural strength of groups C1 ~ C4 was 4.1, 4.4, and 4.2Mpa, 2.2, 2.6, and 2.6Mpa, 1.9, 2.1, and 2.0Mpa, 1.5, 1.5, and 1.5Mpa, respectively, as shown in Fig 8. Average flexural strength of C1, C3 increased firstly and then decreased with the increase of curing time, and the increase and decrease was not significant. With the increase of curing time, the average flexural strength of C2 was increased at 7 and 14 d, and the strength of 14 and 28d was kept constant. The average flexural strength of C4 remained unchanged with the increase of curing time. The above changes are related to curing time and rice husk content.
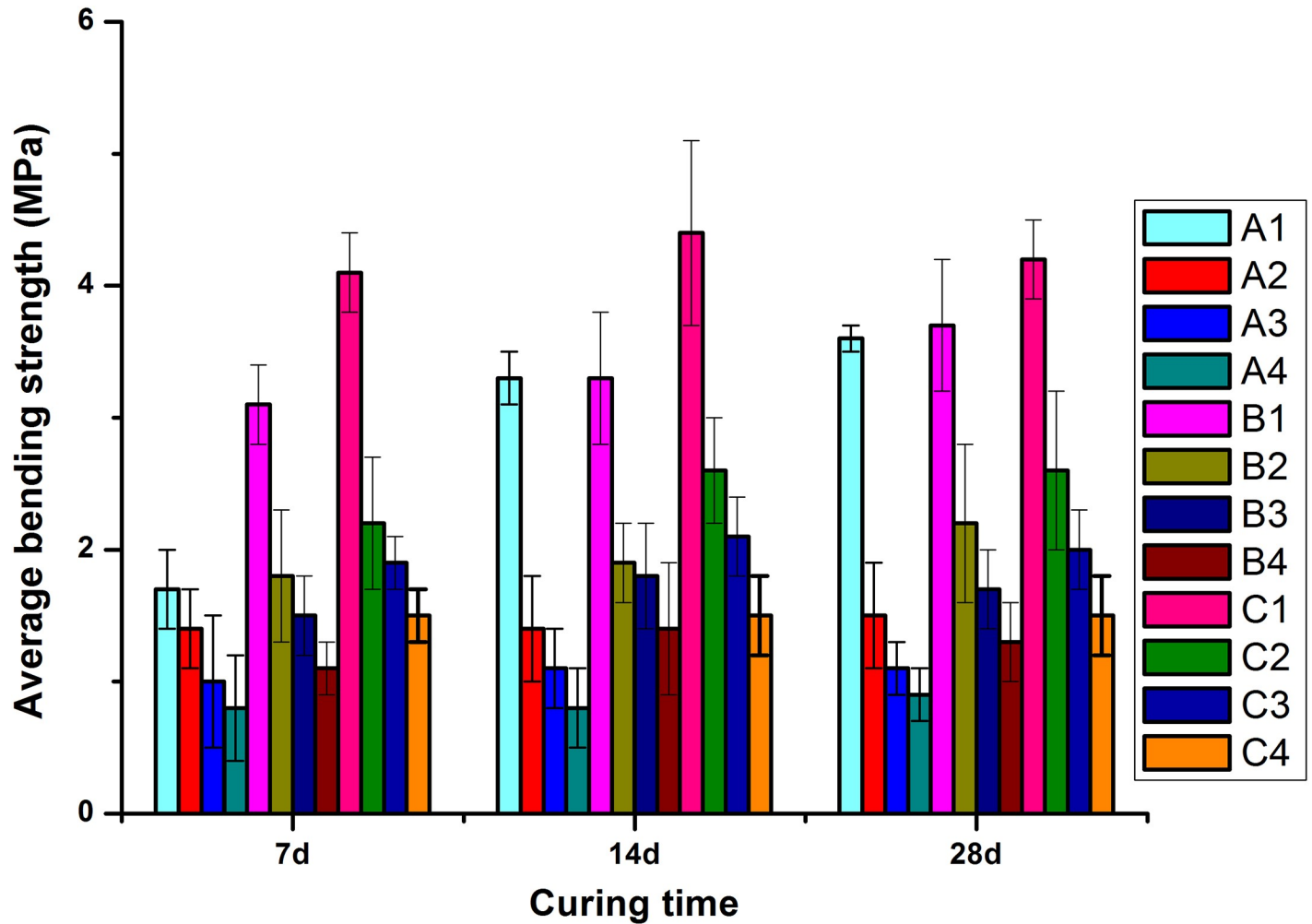
Fig 8. Relationship between curing time and average flexural strength.

In conclusion, average compressive strength and flexural strength of cement-based materials are greatly reduced with the increase of the content of rice husk, and the intensity of 7 ~ 28d is slow or negative when mass of cementitious materials was equal, as shown in Fig 9a. Under the same conditions of curing time, with the increase of the amount of
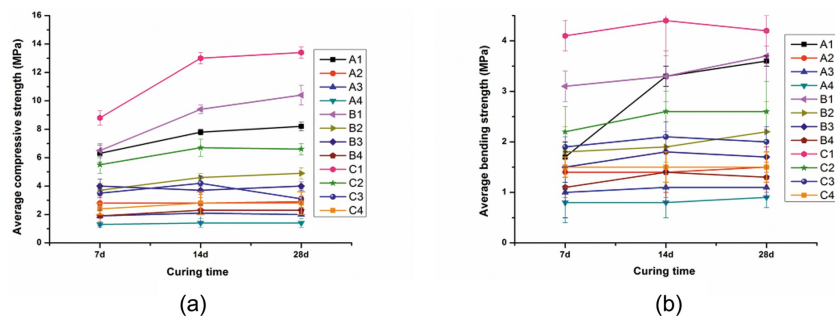

Fig 9. Relationship between curing time and average compressive strength (a), flexural strength (b).

Table 2. Thermal conductivity of test results at 28d.

Number	Cold plate temperature (˚C)	Hot plate temperature (˚C)	Apparent density (Kg/m^3)	Specimen thickness (m)	Thermal conductivity (W/m·˚C)
A1	15	35	1550	0.027	0.1852
A2	15	35	1290	0.027	0.1702
A3	15	35	1220	0.026	0.1433
A4	15	35	1190	0.024	0.1292
B1	15	35	1600	0.026	0.1932
B2	15	35	1450	0.026	0.1997
B3	15	35	1420	0.024	0.1741
B4	15	35	1180	0.025	0.1514
C1	15	35	1680	0.028	0.1958
C2	15	35	1490	0.029	0.1810
C3	15	35	1260	0.026	0.1671
C4	15	35	1230	0.028	0.1239

cementitious material, corresponding to average compressive and flexural strength also increase (Fig 9b).

3.3. Influence of the content of rice husk fiber on thermal conductivity and apparent density of thermal insulation wallboards

The thermal conductivity of thermal insulation wallboards was tested and the results are shown in Table 2. In the absence of rice husk, thermal conductivity λ of A1, B1, and C1 is the largest under 28d of curing time. With the increase of rice hull content, thermal conductivity and apparent density of thermal insulation wallboards decrease correspondingly. Apparent density of thermal insulation wallboards is in range of 1680–1180 Kg/m^3. When the content of rice hull is the largest, the value of thermal conductivity λ is minimum, indicating the better the insulation performance. The average compressive strength of the specimens should be greater than 4.0 MPa according to the actual engineering needs. Fig 8 shows B2 and C2 meet the engineering needs. According to the thermal conductivity, the coefficient of C10 is less than B2, as shown in Table 2. According to test data for C10, thermal insulation wallboards was prepared by mixing river sand (<3mm), cement, fly ash, cellulose ether, and naphthalene superplasticizer, and thermal conductivity of the wallboards 0.9600 W/m·˚C at 28days. In actual engineering, materials with a thermal conductivity of less than 0.20 W/m·˚C are usually called thermal insulation materials. Therefore, C2 can meet certain engineering requirements according to thermal conductivity and strength of thermal insulation wallboards [28–30].

4. Conclusions

Thermal insulation wallboards can well be cast by the mixed slurry of cement, fly ash, cellulose ether, naphthalene superplasticizer, rice hull, and recycled concrete aggregates when slurry consistency was about 8CM. B2 and C2 specimens of compressive strength is bigger than 4MPa, and can be applied to actual engineering. The content of cementitious materials and rice hull has an important influence on the mechanical properties of the resulting thermal insulation wallboards, affecting their application. Average compressive strength, flexural strength, and thermal conductivity of the specimens decreased as the content of rice hull increased. Thermal conductivity of C2 was 0.1810 W/m·˚C less than B2 (0.1997 W/m·˚C) and blank group (0.9600 W/m·˚C) when curing time was 28days. Therefore, C10 will be chosen and used in certain engineering.

Supporting information

S1 Fig. Recycled concrete aggregates.
(TIF)

S1 Table. Chemical composition of the ordinary Portland cement.
(DOCX)

S2 Table. Real content of water.
(DOCX)

Author Contributions

Data curation: Xiaoniu Yu.

Investigation: Xiaoniu Yu.

Methodology: Xiaoniu Yu, Linzhu Sun.

Writing – original draft: Xiaoniu Yu.

Writing – review & editing: Xiaoniu Yu.

References

1. Guedes M, Evangelista L, De Brito J, Ferro A. Microstructural characterization of concrete prepared with recycled aggregates. Microsc Microanal. 2013; 19: 1222–1230. https://doi.org/10.1017/S1431927613001463 PMID: 23673273

2. Li W, Xiao J, Sun Z, Kawashima S, Shah S. Interfacial transition zones in recycled aggregate concrete with different mixing approaches, Constr Build Mater. 2012; 35: 1045–1055. https://doi.org/10.1016/j.conbuildmat.2012.06.022

3. Ferreira L, Brito J, Barra M. Influence of the pre-saturation of recycled coarse concrete aggregates on the fresh and hardened properties of concrete. Mag Concre Res. 2011; 63: 617–627. https://doi.org/10.1680/macr.2011.63.8.617

4. Kou SC, Poon CS. Enhancing the durability properties of concrete prepared with coarse recycled aggregate. Constr Build Mater. 2012; 35: 69–76. https://doi.org/10.1016/j.conbuildmat.2012.02.032

5. Xiao JZ, Li L, Shen LM, Poon CS. Compressive behaviour of recycled aggregate concrete under impact loading. Cement and Concrete Res. 2015; 71: 46–55. https://doi.org/10.1016/j.cemconres.2015.01.014

6. Safiullah O, Elhem G, George W. Relationships between recycled concrete aggregates characteristics and recycled aggregates concretes properties. Constr Build Mater. 2016; 108: 163–174. https://doi.org/10.1016/j.conbuildmat.2016.01.042

7. Vieira T, Alves A, De Brito J, Correia JR, Silva RV. Durability-related performance of concrete containing fine recycled aggregates from crushed bricks and sanitary ware. Mater Design. 2016; 90: 767–776. https://doi.org/10.1016/j.matdes.2015.11.023

8. Reza RS, Bruno D, Renato P, Giovanni D. Properties of cement–lime mortars vs. cement mortars containing recycled concrete aggregates. Constr Build Mater. 2015; 84: 84–94. https://doi.org/10.1016/j.conbuildmat.2015.03.042

9. Thomas C, Setién J, Polanco AJ, Alaejos P, Sánchez de Juan M. Durability of recycled aggregate concrete. Constr Build Mater. 2013; 40: 1054–1065. https://doi.org/10.1016/j.conbuildmat.2012.11.106

10. Wang JY, Vandevyvere B, Vanhessche S, Schoon J, Boon N, Belie ND. Microbial carbonate precipitation for the improvement of quality of recycled aggregates. J Clean Prod. 2017; 156: 355–366. https://doi.org/10.1016/j.jclepro.2017.04.051

11. Hou YQ, Ji XP, Su XL, Zhang WG, Liu LQ. Laboratory investigations of activated recycled concrete aggregate for asphalt treated base. Constr Build Mater. 2014; 65: 535–542. https://doi.org/10.1016/j.conbuildmat.2014.04.115

12. Hanif A, Diao S, Lu Z, Fan T, Li Z. Green lightweight cementitious composite incorporating aerogels and fly ash cenospheres—Mechanical and thermal insulating properties. Constr Build Mater. 2016; 116: 422–430. https://doi.org/10.1016/j.conbuildmat.2016.04.134

13. Duan ZH, Poon CS. Properties of recycled aggregate concrete made with recycled aggregates with different amounts of old adhered mortars. Mater Des. 2014; 58: 19–29. https://doi.org/10.1016/j.matdes.2014.01.044

14. Kang SH, Lee JH, Hong SG, Moon J. Microstructural investigation of heat-treated ultra-high performance concrete for optimum production. Materials (Basel). 2017; 10. https://doi.org/10.3390/ma10091106 PMID: 28930189

15. De Brito J, Ferreira J, Pacheco J, Soares D, Guerreiro M. Structural, material, mechanical and durability properties and behaviour of recycled aggregates concrete. J Build Eng. 2016; 6: 1–16. https://doi.org/10.1016/j.jobe.2016.02.003

16. Yehia S, Helal K, Abusharkh A, Zaher A, Istaitiyeh H. Strength and durability evaluation of recycled aggregate concrete. Int J Concr Struct Mater. 2015; 9: 219–239. https://doi.org/10.1007/s40069-015-0100-0

17. Cardoso R, Silva RV, De Brito J, Dhir R. Use of recycled aggregates from construction and demolition waste in geotechnical applications: A literature review. Waste Manag. 2015; https://doi.org/10.1016/j.wasman.2015.12.021 PMID: 26748436

18. Matias D, De Brito J, Rosa A, Pedro D. Durability of concrete with recycled coarse aggregates : influence of superplasticizers. J Mater Civ Eng. 2014; 06014011: 1–5. https://doi.org/10.1061/(ASCE)MT.1943-5533.0000961

19. De Brito J, Saikia N. Recycled aggregate in concrete use of industrial, Construction and Demolition Waste. 2013.

20. Hanif A, Kim Y, Lu Z, Park C. Early-age behavior of recycled aggregate concrete under steam curing regime. J Clean Prod. 2017; 152: 103–114. https://doi.org/10.1016/j.jclepro.2017.03.107

21. Guedes M, Evangelista L, de Brito J, Ferro AC. Microstructural characterization of concrete prepared with recycled aggregates. Microsc Microanal. 2013; 19: 1222–1230. https://doi.org/10.1017/S1431927613001463 PMID: 23673273

22. Rao S, Silva P, De Brito J. Experimental study of the mechanical properties and durability of self-compacting mortars with nano materials (SiO$_2$ and TiO$_2$). Constr Build Mater. 2015; 96: 508–517. https://doi.org/10.1016/j.conbuildmat.2015.08.049

23. Pedro D, De Brito J, Evangelista L. Performance of concrete made with aggregates recycled from precasting industry waste: influence of the crushing process. Mater Struct. 2015; 48: 3965–3978. https://doi.org/10.1617/s11527-014-0456-7

24. Pedro D, De Brito J, Evangelista L. Evaluation of high-performance concrete with recycled aggregates: Use of densified silica fume as cement replacement, Constr Build Mater. 2017; 147: 803–814. https://doi.org/10.1016/j.conbuildmat.2017.05.007

25. Li WG, Luo ZY, Tao Z, Duan WH, Shah SP. Mechanical behavior of recycled aggregate concrete-filled steel tube stub columns after exposure to elevated temperatures. Constr Build Mater. 2017; 146: 571–581. https://doi.org/10.1016/j.conbuildmat.2017.04.118

26. Ignjatovic IS, Marinkovic SB, Tošic N. Shear behaviour of recycled aggregate concrete beams with and without shear reinforcement. Eng Struct. 2017; 141: 386–401. https://doi.org/10.1016/j.engstruct.2017.03.026

27. Sadati S, Arezoumandi M, Khayat KH, Volz JS. Shear performance of reinforced concrete beams incorporating recycled concrete aggregate and high-volume fly ash. J Clean Prod. 2016; 115: 284–293.

28. Hanif A, Parthasarathy P, Li Z. Utilizing fly ash cenosphere and aerogel for lightweight thermal insulating cement-based composites. ICGBMCE 2017 : 19th International Conference on Green Building, Materials and Civil Engineering, London, United Kingdom February 16–17, 2017.

29. Yun TS, Jeong YJ, Han TS, Youm KS. Evaluation of thermal conductivity for thermally insulated concretes. Energy Build. 2013; 61: 125–132. https://doi.org/10.1016/j.enbuild.2013.01.043

30. Demirboğa R, Gül R. Thermal conductivity and compressive strength of expanded perlite aggregate concrete with mineral admixtures. Energy Build. 2003; 35: 1155–1159. https://doi.org/10.1016/j.enbuild.2003.09.002